



Long non-coding RNA DSCAS regulates cisplatin sensitivity in lung squamous cell carcinoma by competitively binding to miR-646-3p

Hongping Liu^{a,b,1}, Chunya Lu^{a,1}, Ping Li^a, Hongxia Jia^a, Yan Wang^a,
Jiuling Cheng^a, Ruirui Cheng^a, Guojun Zhang^{a,*}

^a Department of Pulmonary and Critical Care Medicine, The First Affiliated Hospital of Zhengzhou University, No.1, Jianshe East Road, Zhengzhou, Henan 450052, PR China

^b Academy of Medical Sciences, Zhengzhou University, Zhengzhou, China

ARTICLE INFO

Keywords:

LncRNA DSCAS
miR-646-3p
Lung squamous cell carcinoma
Cisplatin sensitivity

ABSTRACT

Background: Platinum-based chemotherapy is the main treatment for advanced lung squamous cell carcinoma (LUSC). Eventually, patients with LUSC develop resistance to cisplatin, which affects the prognosis. Hence, the researchers sought to find a lncRNA in LUSC that affects resistance to cisplatin.

Methods: The lncRNA microarray assay was used to screen the differential expression of lncRNA. qPCR was used to detect lncRNA DSCAS (DSCAS) expression in tissues and cell lines. Lentiviral transfection was used to regulate the expression of DSCAS. CCK-8, colony formation, wound healing, transwell, and flow cytometry assays were used to assess the biological behaviors and sensitivity to cisplatin of LUSC cell. RNA-RNA interaction was tested using the dual luciferase reporting assay, RNA-IP, and RNA-RNA pull-down assay. The downstream pathway of DSCAS was verified by qPCR and Western blotting assays.

Results: DSCAS was highly expressed in LUSC tissues and cells, and its expression levels were higher in cisplatin-insensitive tissues than in cisplatin-sensitive tissues. Elevation of DSCAS promoted cell proliferation, migration and invasion as well as increased cisplatin resistance of lung cancer cells, while demotion of DSCAS inhibited cell proliferation, migration and invasion as well as decreased the cisplatin resistance of lung cancer cells. DSCAS bound to miR-646-3p to regulate the expression of Bcl-2 and Survivin, which affected the cell apoptosis and sensitivity to cisplatin in LUSC cells.

Conclusions: DSCAS regulates biological behavior and cisplatin sensitivity in LUSC cells by competitively binding to miR-646-3p to mediate the expression of Survivin and Bcl-2, known as apoptosis-related proteins.

1. Introduction

With a high global morbidity and fatality rate, lung cancer is one of the most aggressive cancers and ranks second in the incidence of male and female malignant tumors, next only to prostate cancer and breast cancer, respectively. However, lung cancer mortality ranks

* Corresponding author.

E-mail address: zgj@zzu.edu.cn (G. Zhang).

¹ Hongping Liu and Chunya Lu contributed equally to this work.

first in both male and female tumors [1]. Eighty to eighty-five percent of lung cancer diagnoses are non-small cell lung cancer (NSCLC), of which the most prevalent pathologic kinds are lung adenocarcinoma (LUAD) and lung squamous cell carcinoma (LUSC) [2,3]. The emergence of targeted therapy is a milestone in the development of lung cancer treatment, which significantly extends the survival period and improves the patients' quality of life. Most targeted drug applications are focused on LUAD [4–8], but unfortunately, the efficacy of targeted therapy in patients with LUSC has not been optimistic [9,10]. Platinum-based doublet therapy (for instance, cisplatin in conjunction with another cytotoxic medication) and immunotherapy remain the mainstay of treatment for advanced, unresectable squamous lung cancer [11]. However, the clinical response is often limited by the inherent or acquired chemotherapeutic drug resistance [12]. Hence, understanding the underlying mechanism of cisplatin resistance in lung squamous cell carcinoma is critical to enhance chemotherapy effectiveness and improve survival outcomes for patients with LUSC.

Non-coding RNAs (ncRNAs) perform a wide range of biological roles. They include long non-coding RNA (lncRNA), microRNA (miRNA), small interfering RNA (siRNA), and Piwi interaction RNA (piRNA), and so on, which affect gene expression at the transcription, RNA processing, and translation levels [13,14]. LncRNAs are RNA molecules that have more than 200 nucleotides but little or no capacity to encode protein [15], which can regulate gene expression through cis or trans, with mRNA-like structure, polyA tail, and promoter structure [16]. However, the regulation mechanism of lncRNA is not well understood [17]. In competitive endogenous RNA (ceRNA) mechanism, lncRNA was considered as a type of ceRNA, which can competitively bind to miRNA and inhibit the effect of miRNA in the negative regulation of target gene mRNA [18], further participating in the control of other signaling pathways and biological functions [19–22]. The majority of the interactions between miRNAs and the mRNA 3' untranslated regions (3'UTR) are in a complete or incomplete complementary binding mode to control the expression of their target genes at both post-transcriptional and translational stages [23]. Currently, there are more than 70,000 experimentally verified lncRNAs interacting with miRNAs in relevant databases [24]. Previous studies have indicated that some differentially expressed lncRNAs in lung cancer and other tumors, such as HOTAIR, UCA1, and BLACAT1, were involved in cell invasion, metastasis, proliferation, apoptosis, chemotherapy sensitivity, even the survival and prognosis of patients [25–27].

We identified differentially expressed lncRNAs between cisplatin-sensitive and cisplatin-insensitive LUSC patients by lncRNA microarray assay. To clarify the molecular mechanism of a specific lncRNA in cisplatin resistance of LUSC cells, we performed gain- and loss-of-function studies of the differentially lncRNA and validated the downstream molecular pathway.

2. Materials and methods

2.1. Experimental design and samples

All tissue samples were obtained from male patients with LUSC who were hospitalized in the First Affiliated Hospital of Zhengzhou University from January 2020 to December 2021. A total of 63 pairs of LUSC tissues and adjacent normal tissues were acquired from patients who underwent tumour resection. The adjacent normal tissues were the normal lung tissue more than 5 cm away from the focus. A total of 55 cases of chemotherapy-sensitive LUSC tissues and 55 cases of chemotherapy-insensitive LUSC tissues were obtained from CT-guided percutaneous puncture or bronchoscopic biopsy. The two groups of patients were matched according to age and TNM stage. The basic characteristics of the patients are shown in Table 1. Evaluation criteria for chemotherapy sensitivity: Patients were followed up to 2 cycles of chemotherapy according to RECIST 1.1 (Response Evaluation Criteria in Solid Tumors). CR, PR, and SD were considered as chemosensitivity, and PD was considered as chemoresistance.

Specific inclusion criteria were as follows:

- The cancer tissue was histologically confirmed as LUSC without necrosis.
- No other cancers were diagnosed except lung cancer.
- Informed consent was obtained and signed by the patient or family.

The exclusion criteria were as follows:

- The patient was lost to follow-up.
- The total amount of each sample block is less than 100 mg.

Table 1

Character summaries of 173 LUSC cases.

Specimen	Age, y		TNM stage	
	≥60	<60	I ~ II	III ~ IV
Surgery resection LUSC/normal (paired specimen), n (%)	27 (42.9%)	36 (57.1%)	53 (84.1%)	10 (15.9%)
CT-guided percutaneous puncture/bronchoscopic biopsy				
Chemotherapy-sensitive, n (%)	37 (67.3%)	18 (32.7%)	19 (34.5%)	36 (65.5%)
Chemotherapy-insensitive, n (%)	32 (58.2%)	23 (41.8%)	21 (38.2%)	34 (61.8%)
Total	96	77	93	80

LUSC: lung squamous cell carcinoma.

See Fig. 1 for a flowchart of the experimental design. All clinical operations adhered to the Declaration of Helsinki's principles. The First Affiliated Hospital of Zhengzhou University's institutional ethics committee gave its approval for this study. Ethics No.:2021-KY-0302.

2.2. Cells and reagents

The normal human bronchial epithelial (NHBE) cell line and lung squamous cell carcinoma H520 and SK-MES-1 cell lines were acquired from the Shanghai Institutes for Biological Sciences' China Center for Type Culture Collection (CCTCC) (Shanghai, China). Sigma- Aldrich (St. Louis, MO, USA) provided cisplatin (CAS:15663-27-1).

2.3. LncRNA microarray assay

The total RNAs of cisplatin-sensitive, cisplatin-insensitive, and adjacent normal tissues were extracted, and the lncRNA microarray assay was conducted. The Agilent Bioanalyzer 2100 (Agilent Technologies, Santa Clara, CA, USA) was used to determine the integrity of the RNA. Following the manufacturer's instructions, samples were labelled, hybridised to microarrays, and washed. The Agilent Scanner G2505C (Agilent Technologies) was used to scan the arrays. Feature Extraction software (version 10.7.1.1, Agilent Technologies) was used to get raw data and array pictures. The basic raw data was analyzed through GeneSpring (version 13.1, Agilent Technologies). The fold change was used to determine lncRNAs differentially expressed, and the *t*-test was used to obtain the *P*-values. The significance of differential expression was determined by the fold change of 2.0 and a *P*-value $\leq .05$. To exhibit distinct lncRNA expression patterns across samples, hierarchical clustering was used.

2.4. Cell culture

Lung squamous cell carcinoma cell line (H520, SK-MES-1) and normal human bronchial epithelial cell line (NHBE) were cultured for subsequent experiments. 90% medium +10% FBS +1% streptomycin and penicillin were used in the cell culture environment, which was maintained at 37 °C, 5% CO₂, and 95% saturated humidity. At regular intervals, the culture medium was changed, and the cells were passaged at a density of around 70–90%.

2.5. Cell transfection

For stably transfected cells, SK-MES-1 cells were seeded in 6-well plates at a density of 3.5×10^5 cells/well. When cell growth density reached 70%, cells were treated with polybrene (work concentration = 4 μ g/ml) and co-transfected with lentiviral vectors (MOI = 70) containing DSC1/DSC2 antisense RNA (DSCAS) overexpression (oe-DSCAS), DSCAS overexpression negative control (oe-NC), DSCAS short hairpin RNA (sh-DSCAS) or DSCAS short hairpin RNA negative control (sh-NC), respectively. HANBIO Co, Ltd (Shanghai, China) created the lentiviruses described above. Fluorescent microscope was used to assess the transfection efficiency, and 2 μ g/ml puromycin was used to screen the stable expressed cells.

For transient transfected cells, at a density of 3.5×10^5 cells/well, SK-MES-1 cells were planted in 6-well plates and were co-transfected with the miR-646-3p mimics/mimics negative control (mimics NC) (Shanghai GenePharma Co. Ltd. Shanghai, China), and Lipofectamine 3000 (Thermo, USA) according to manufacturer's protocol. GenePharma (Shanghai, China) generated the RNA sequences. (Table 2).

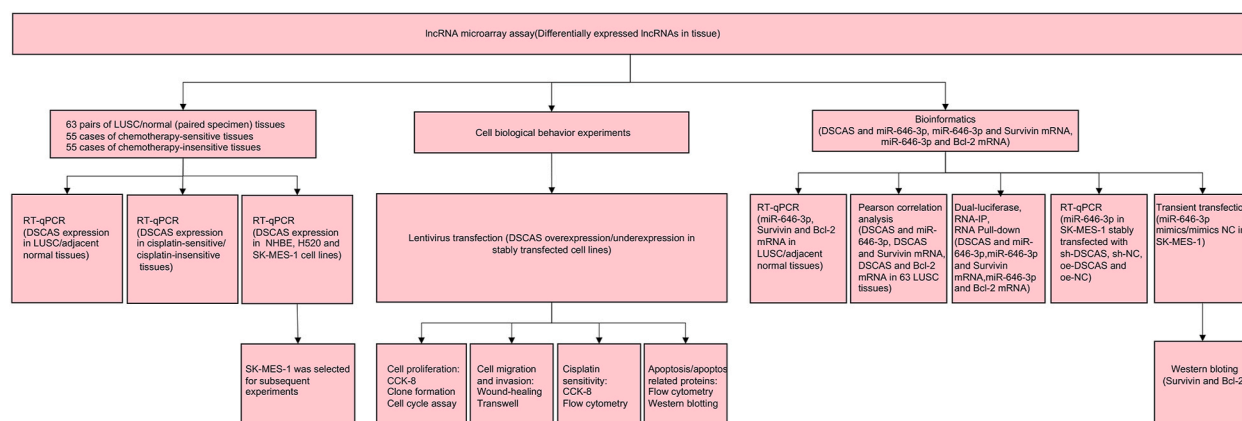


Fig. 1. The brief flow chart of the experimental design.

2.6. Real-time quantitative reverse transcription PCR (RT-qPCR)

Total RNA was extracted using Trizol (15596026, Invitrogen). Following the manufacturer's instructions, DSCAS was reverse transcribed to cDNA using the RevertAid First Strand cDNA Synthesis Kit (K1622, Thermo). The sample was fed into a quantitative real-time PCR device (Applied Biosystems: 7500, Thermo Fisher Scientific) using a Maxima SYBR Green qPCR Master Mix (2X), (K0251, Thermo). Using the $2^{-\Delta\Delta Ct}$ method, the relative amount of lncRNA expression was quantified and standardised to glyceraldehyde-3-phosphate dehydrogenase (GAPDH). MiRNA-646 was reversely transcribed and underwent quantitative polymerase chain reaction using Hairpin-it™ microRNA and U6 snRNA Normalization RT-PCR Quantitation Kit (GenePharma, Shanghai, China), in accordance with the manufacturer's instructions.

Sangon (Shanghai, China) and GenePharma (Shanghai, China) created the primers. (Table 3).

2.7. Wound-healing assay

The 6-well plate was seeded with 2.5×10^5 cells/well stably transfected cells in the logarithmic growth phase. With the use of a tip, the monolayer was scraped, and any detached cells were then washed away with phosphate buffered saline. The cells were then cultivated in full media and captured in photographs at 0 and 24 h after injury. The migration area (%) = $(A_0 - A_n)/A_0 \times 100$ formula was used to determine the wound closure rate. A_0 stands for the original wound area, and A_n for the residual area at the metering point.

2.8. Colony formation assay

The cells were sown onto a 6-well plate (approximately 200 cells/well) during the logarithmic growth phase by a multiple dilution method following cell digestion. After incubation (37 °C, 5% CO₂, and 95% saturated humidity; 14 d), cells were fixed with 4% paraformaldehyde (leagene biotechnology, China) and stained with 0.1% crystal violet (leagene biotechnology, China). Formed colonies were taken pictures with a digital camera and counted manually.

2.9. Cell counting kit-8 (CCK-8) assay

For cell proliferation assay, four groups of SK-MES-1 cell lines stably transfected with oe-DSCAS, oe-NC, sh-DSCAS, and sh-NC respectively, were digested and seeded onto 96-well plates (3000 cells/well). At the time point of 0, 24, 48, 72h, 10 µl of CCK-8 solution (CK04-500, Dojindo) was added to the cells for detection. A microplate reader (SpectraMax i3x, Molecular Devices, USA) was used to measure the optical density (OD) value at 450 nm after the plate had been incubated for 2 h in the incubator. Three wells in each group were subjected to statistical analysis, and GraphPad Prism 9 for Mac (Version 9.3.1) was used to design a growth curve in accordance with the results.

For the cell proliferation toxicity assay, each group of SK-MES-1 cell lines stably transfected were seeded into 96-well plates after being digested (5000 cells/well). After adherence, cells were given different concentration of cisplatin (0, 1, 2, 4, 8, 16, 32, 64, 96, 128 µM) and culture was continued for 24 h. CCK-8 solution (CK04-500, Dojindo, 10 µl added) was incubated in the cell culture medium for 2 h. To determine the optical density (OD) value at 450 nm wavelength, the plate was placed in a microplate reader (SpectraMax i3x, Molecular Devices, USA). Each group's three wells underwent statistical analysis and using GraphPad Prism 9 for macOS (Version 9.3.1), the curve of 50% inhibitive concentrations (IC₅₀) of cisplatin was then produced.

2.10. Transwell assay

For the invasion assay, matrigel (356234, BD Biosciences, USA) was diluted to 300 µl/ml in serum-free medium at 4 °C. Diluted matrigel was applied to the membrane's top surface in the transwell chamber before the membrane was incubated for 30 min at 37 °C. After adding 700 µl cell culture medium with 20% serum to the lower chamber, 100 µl serum-free RPMI1640 medium contained with 2×10^4 cells were placed in one well of the 24-well transwell upper chamber (Corning Costar). After 24 h of incubation, invaded cells were fixed with 4% paraformaldehyde (leagene biotechnology, China) and stained with 0.1% crystal violet (leagene biotechnology, China) while the noninvaded cells were removed using a cotton swab. Under an inverted light microscope, the number of invading cells was manually counted in three randomly chosen regions (LEICA DFC450C, Germany).

For the migration assay, it was the same as the invasion assay, except that there was no matrigel on the upper chamber.

Table 2
RNA sequences used for transient transfection.

Target	RNA sequences (5'-3')
has-miR646 mimics	sense: 5'-AAGCAGCUGCCUCUGAGGC -3' antisense: 5'-CUCAGAGGCAGCUGCUUUU-3'
Mimics NC	sense: 5'-UUCUCCGAACGUGUCACGUTT -3' antisense: 5'-ACGUGACACGUUCGGAGAATT -3'

NC: negative control.

Table 3
Primer sequences used for RT-qPCR.

Target	Primer sequences (5'–3')
lncRNA DSCAS	F: 5'-TGCGCTGATTACATCTACCG -3' R: 5'-TAAGTCTCAGTCTTCAAGCCT-3'
Survivin	F: 5'-AAGAACTACCGCATCGCCACC -3' R: 5'-AGCCAGCTCCGCCATT -3'
Bcl-2	F: 5'-GGATGCCTTTGTGGAAAACCTGT -3' R: 5'-AGCCTGCAGCTTTGTTTCAT -3'
GAPDH	F: 5'-CCGGAAACTGTGGCGTGATGG -3' R: 5'-AGGTGGAGGAGTGGGTGTCGCTGTT -3'
has-miR-646	F: 5'-GGTTGCGTTAAGCAGCTGC -3' R: 5'-TATGGTTCTTCACGACTGGTTCAC-3'
U6	F: 5'-CAGCACATATACTAAAATTGGAACG -3' R: 5'-ACGAATTTGCGTGCATCC-3'

GAPDH: glyceraldehyde-3-phosphate dehydrogenase. F: Forward primer. R: Reverse primer.

2.11. Western blotting analysis

Utilizing RIPA lysate (R0010, Solarbio) augmented with PMSF, total protein was lysed and collected. The supernatant was obtained after the proteins had been centrifuged at 8000 g for 5 min at 4 °C after being incubated on ice for 30 min. A protein quantification kit from Solarbio called BCA (PC0020) was used to confirm the protein content. 500 µg of protein were collected in all and dissolved in SDS loading buffer. Proteins were separated by SDS-PAGE Gel electrophoresis and transferred to PVDF membrane after boiling at 100 °C for 5 min. NcmBlot blocking buffer (P30500, NCM Biotech) was used to block the membrane for 10 min at room temperature. After that, the membrane was incubated with diluted primary antibodies from Cell Signaling Technology (CST) for Bcl-2 (1: 1000, D55G8), Survivin (1: 1000, 71G4B7), Bax (1: 1000, D3R2M), Caspase-3 (1: 1000, 9662), Cleaved Caspase-3 (1: 1000, Asp175), and β-Actin (internal reference; 13E5, 1: 1000) overnight at 4 °C. Horseradish peroxidase-labelled goat anti-rabbit secondary antibody Immunoglobulin G (IgG) (1:2000, 7074, CST) was used to reprobe the membrane for 1 h at room temperature. Following processing, a chemiluminescence fluorescence detection kit (NcmECL Ultra, NCM Biotech) was used to incubate the membrane. The membrane was captured with the camera using a GE Amersham Imager 680 image analysis equipment, and the program ImageJ version 1.53 was used to evaluate the picture's gray scale.

2.12. Flow cytometry

For the cell cycle assay, cell cycle was examined using a cell cycle detection kit (KGA512, KeyGEN BioTECH, Nanjing, China). Prior to application, Rnase A: PI working solution was prepared by dyeing working solution by 1:9 volume. After the cells were gathered, the cell concentration was changed to 1×10^6 cells per milliliter. 1 ml of single cell suspension was centrifuged, the supernatant was removed, and 500ul of 70% cold ethanol was added into the cells for fixation (2 h to overnight). Before dyeing, the fixative was removed with PBS and stored at 4 °C. Add 500 µL PI/Rnase A staining solution prepared in advance, keeping away from light for 30–60min at room temperature. The cells were put into a flow cytometer (BD FACSCelesta, BD Biosciences, USA.) Record red fluorescence at an excitation wavelength of 488 nm. The results were plotted and analyzed applying FlowJo10.4 software.

For cell apoptosis assay, the apoptosis rate of stably transfected cell lines was assessed using the Annexin V-APC/PI Apoptosis Detection Kit (KeyGEN BioTECH, Nanjing, China; KGA1030-100). Each type of SK-MES-1 cells stably transfected was seeded on 6-well plates (3.5×10^5 cells/well) and cultured with 20 µM cisplatin for 24 h. Trypsin without EDTA was used to digest cells in 6-well plates. The samples were centrifuged at 2000 rpm for 5 min, using PBS to clean twice. 500 µl of Binding Buffer was added to suspend the cells after the PBS was taken out. PI (5 µl) and annexin V-APC (5 µl) were added. After 15 min of standing at room temperature in the dark, the flow cytometer was used to detect a fluorescence signal in the relevant channel. In order to distinguish between cells in normal conditions, early apoptosis, late apoptosis, and death, flow cytometry (BD FACSCelesta, BD Biosciences, USA) was utilized. Finally, the apoptosis rate of cells was plotted and analyzed using FlowJo10.4 software.

2.13. Dual luciferase reporter gene assay

The connection between DSCAS and miR-646-3p was examined using a dual-luciferase reporter experiment, and it was determined if Bcl-2 and Survivin were the miR-646-3p target genes. Promega (Madison, WI, USA) provided the pmirGLO vector for purchase. Shanghai Biological Technology Company (Shanghai, China) created recombinant vectors with sequences of both wild-type (pmirGLO-Wt- DSCAS 3'UTR, pmirGLO-Wt-Bcl-2 3'UTR, and pmirGLO-Wt-Survivin 3'UTR) and mutant-type (pmirGLO-Mut-DSCAS 3'UTR, pmirGLO-Mut-Bcl-2 3'UTR and pmirGLO-Mut-Survivin 3'UTR). Cotransfection of recombinant vectors and miR-646-3p mimics or miR-scramble into SK-MES-1 cells. Using a luciferase assay kit from Promega, Madison, WI, USA, and a luminescence microplate reader, luciferase activity was assessed 24 h after cotransfection and normalized to the activity of Renilla luciferase (Berthold, Bad Wildbad, Germany). The experiments were carried out three times.

2.14. RNA immunoprecipitation (RNA-IP) assay

RNA-IP experiments were done with EZ-Magna RIP Kit (Millipore, USA) following the manufacturer’s instruction. Firstly, cells were collected and lysed in complete RIP lysis buffer. The precipitate was discarded by centrifugation at 14,000 g for 10min at 4 °C, and the supernatant was retained. Then, the cell extract was incubated with RIP buffer containing magnetic beads conjugated to a human anti-Ago2 antibody (Millipore, USA). 500 µl of washing buffer was added to each EP tube and gently shaken. Then samples were centrifuged at 10,000g for 2min. Wash three times in total. Trizol was added and total RNA was extracted according to the RNA extraction method. RT-qPCR was performed to verify the expression of RNA.

2.15. RNA pull-down assay

Biotin-labelled RNA was transcribed with Biotin RNA Labeling Mix (Roche) and T7 polymerase (Promega) and then treated with purified Rneasy Mini Kit (QIAGEN). The RNA probes were mixed with SK-MES-1 cell lysates for 3h at 4 °C, and the complexes were then mixed with streptavidin magnetic beads (Thermo Fisher Scientific) for 2 h. Finally, RT-qPCR was used to verify the expression level of the target RNA binding to miR-646-3p.

2.16. Statistical analysis

Statistical data were processed and analyzed using SPSS 26.0 (IBM Corp.) and Prism 9.3.1 for macOS (GraphPad LLC). The mean and standard deviation of at least three independent tests were used to describe the measurement data. For comparison between two groups, the *t*-test was used. To compare three or more groups, a one-way analysis of variance (ANOVA) was performed, and post hoc pairwise comparisons were used with the least significant difference (LSD) *t*-test. The normal probability conversion method and nonlinear regression analysis were used to determine the IC50 of cisplatin. Statistical significance was defined as a *P*-value of < .05.

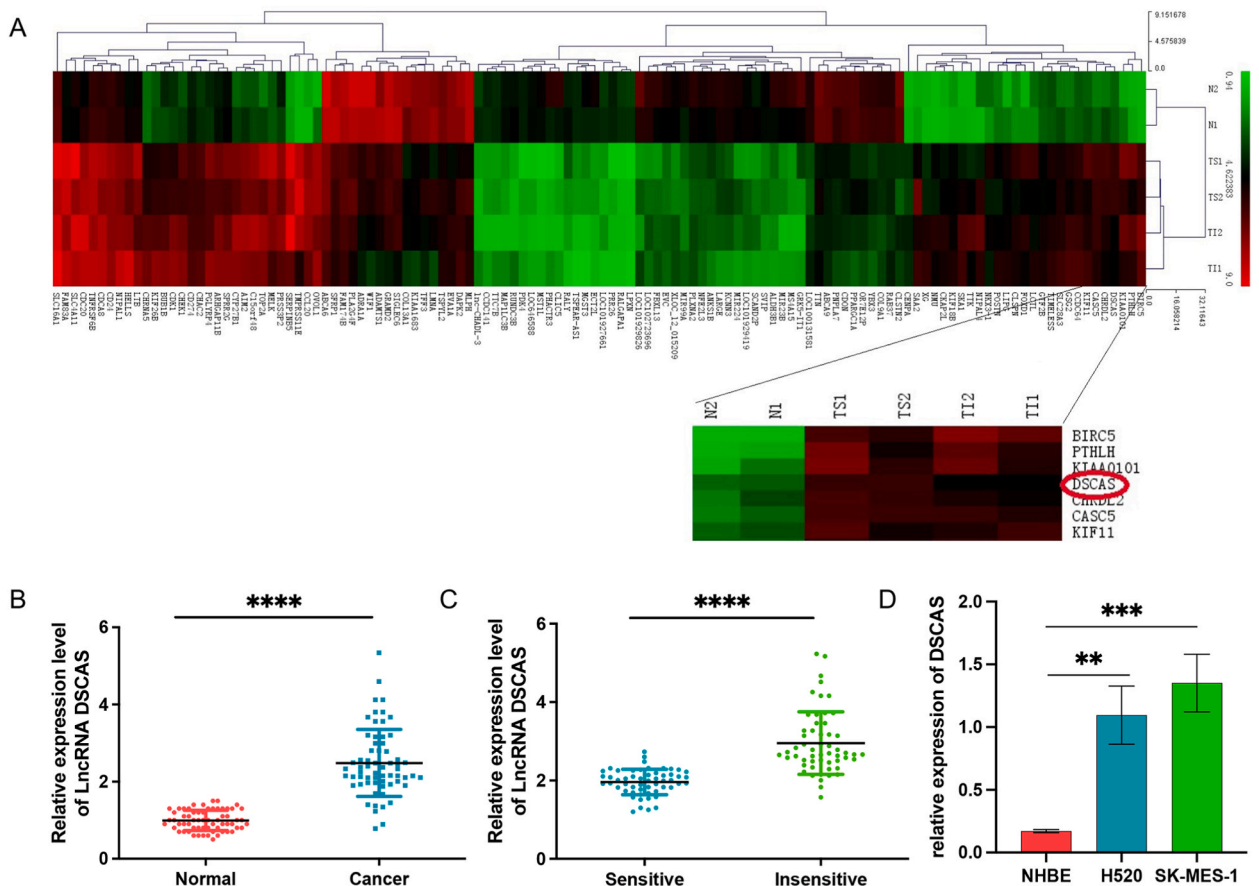


Fig. 2. DSCAS was screened and validated in tissues and cell lines. (A). The differential expression of lncRNA among normal adjacent tissues, cisplatin-sensitive and cisplatin-insensitive lung squamous carcinoma tissues were screened using gene chip. (Fold change >2.0, *P* < .05). (B–C). DSCAS expression was validated in lung tissues by RT-qPCR assay. (*P* < .05). (D). DSCAS expression was validated in cell lines by RT-qPCR assay. (*n* = 3, *P* < .05). **P* < .05, ***P* < .01, ****P* < .001 , *****P* < .0001 compared with control.

3. Results

3.1. DSCAS was highly expressed in LUSC tissues and cells and was higher in cisplatin-insensitive tissues

Gene chip assay was used to identify the differential expression of lncRNA in 6 LUSC specimens (2 cisplatin-insensitive, 2 cisplatin-sensitive, and 2 adjacent normal tissues, respectively). Microarray results showed that DSCAS was abnormally high in LUSC tissues and higher in cisplatin-insensitive tissues than in cisplatin-sensitive tissues (Fold change >2.0, $P < .05$; Fig. 2A). RT-qPCR assay was adopted to estimate the expression of DSCAS in LUSC tissues and cell lines. The expression of DSCAS was strikingly higher in LUSC tissues compared to normal tissues. ($n = 63, P < .05$; Fig. 2B). DSCAS expression in cisplatin-insensitive tissues was higher than that in

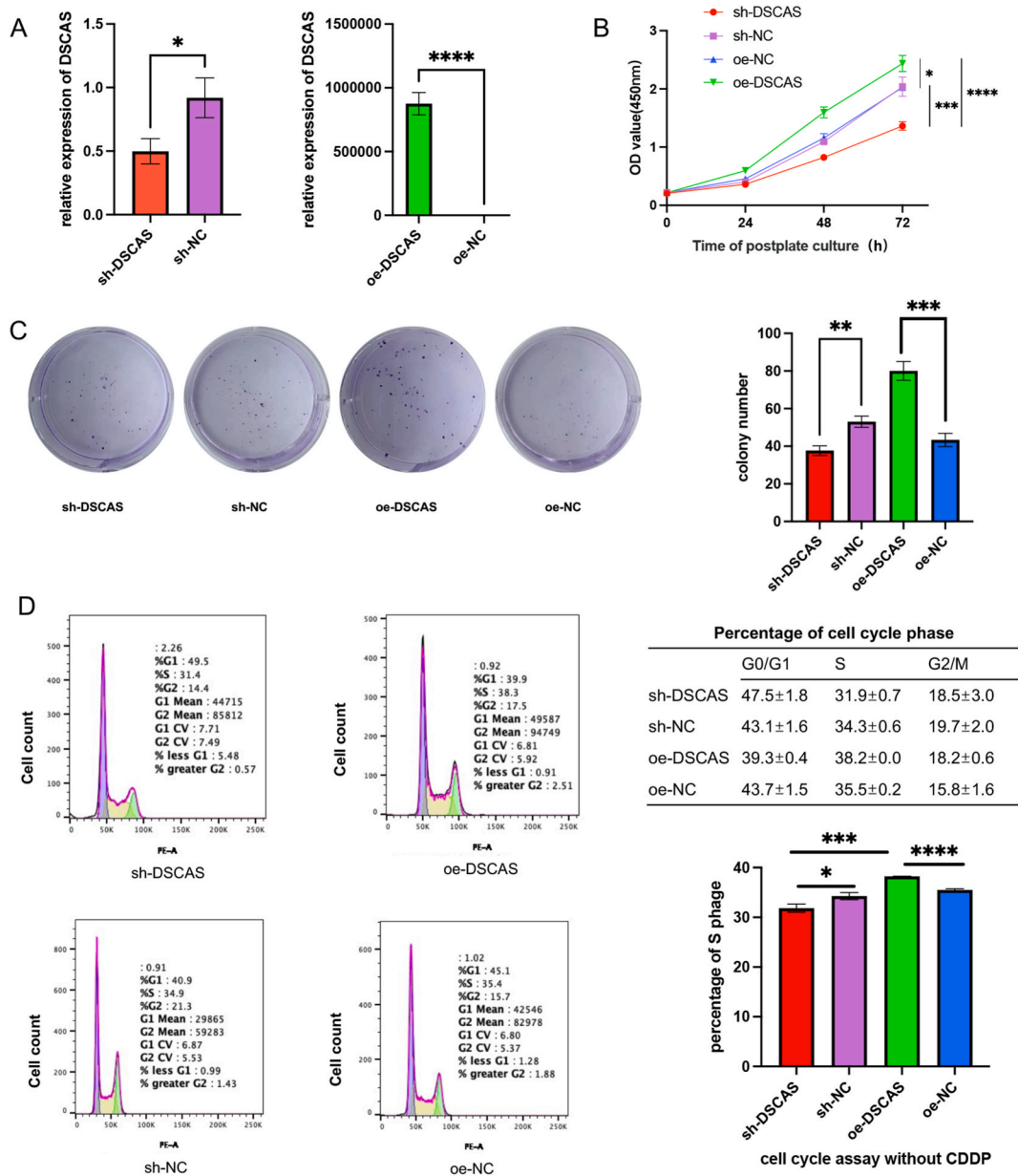


Fig. 3. Effects of regulating DSCAS on the proliferation of SK-MES-1 cells. (A). DSCAS was up- and down-regulated in SK-MES-1 cells by lentiviral vectors transfection. The relative expression of DSCAS was confirmed applying RT-qPCR assay. ($n = 3, P < .05$). (B). CCK-8 assay indicated that SK-MES-1 cells harboring oe-DSCAS exhibited highest proliferation ability, while SK-MES-1 cells harboring sh-DSCAS showed the lowest proliferation ability. ($n = 3, P < .05$). (C). Cell proliferation was validated by colony formation assay. ($n = 3, P < .05$). (D). Cell cycle assay revealed that SK-MES-1 cells harboring oe-DSCAS possessed the highest proportion of S phase which indicates the proliferation ability of cells, while the proportion of S phase of SK-MES-1 cells harboring sh-DSCAS was lowest. ($n = 3, P < .05$). * $P < .05$, ** $P < .01$, *** $P < .001$, **** $P < .0001$ compared with control.

cisplatin-sensitive tissues. ($n = 55, P < .05$; Fig. 2C). To further validate its differential expression, DSCAS was assessed in LUSC cell lines (H520 and SK-MES-1) and normal human bronchial epithelial cell line (NHBE) using RT-qPCR assay, revealing a similar result consistent with tissues. ($n = 3, P < .05$; Fig. 2D). The aforementioned data were indicative of a high expression pattern of DSCAS in both lung squamous carcinoma tissues and cells, especially in cisplatin-insensitive tissues.

3.2. Regulation of DSCAS altered cell proliferation

To elucidate the biological behavior of cells after regulating DSCAS, DSCAS was overexpressed in SK-MES-1 cell line by transfecting lentiviral vectors containing oe-DSCAS, and oe-NC was acted as control; meanwhile, DSCAS was also underexpressed via lentiviral vectors containing sh-DSCAS, and sh-NC was used as control. Transfected efficiency was confirmed using RT-qPCR assay. ($n = 3, P < .05$; Fig. 3A). The CCK-8 assay suggested that the cell proliferation capacity of sh-DSCAS group was lower than that of sh-NC group, and that of oe-DSCAS group was higher than that of oe-NC group ($n = 3, P < .05$; Fig. 3B). The clonal formation assay indicated that the number of clones formed in sh-DSCAS group was lower than that in sh-NC group, and the number of clones formed in oe-DSCAS group was higher than that in oe-NC group ($n = 3, P < .05$; Fig. 3C). The cell cycle assay showed that the proportion of S-phase cells in sh-DSCAS group was lower than that in sh-NC group, and the proportion of S-phase cells in oe-DSCAS group was higher than that in oe-NC group ($n = 3, P < .05$; Fig. 3D). These data displayed that DSCAS overexpression significantly increased the proliferation of SK-MES-1 cells, while DSCAS underexpression surely inhibited proliferation of SK-MES-1 cells.

3.3. Modulation of DSCAS affected cell migration and invasion

Wound-healing and transwell for migration and invasion assays were performed using stably transfected SK-MES-1 cell lines. Wound-healing assay indicated SK-MES-1 cells harboring oe-DSCAS had the higher wound closure rate in comparison to oe-NC group, while the wound closure rate of sh-DSCAS group was lower than that in sh-NC group. ($n = 3, P < .05$; Fig. 4A). Transwell assays with or without Matrigel both showed SK-MES-1 cells carrying oe-DSCAS had more transmembrane cells, while SK-MES-1 cells carrying sh-DSCAS had less transmembrane cells when compared to their respective control groups. ($n = 3, P < .05$; Fig. 4B–C). These results suggested that DSCAS overexpression in SK-MES-1 cell lines promoted cell migration and invasion, while DSCAS underexpression inhibited cell migration and invasion.

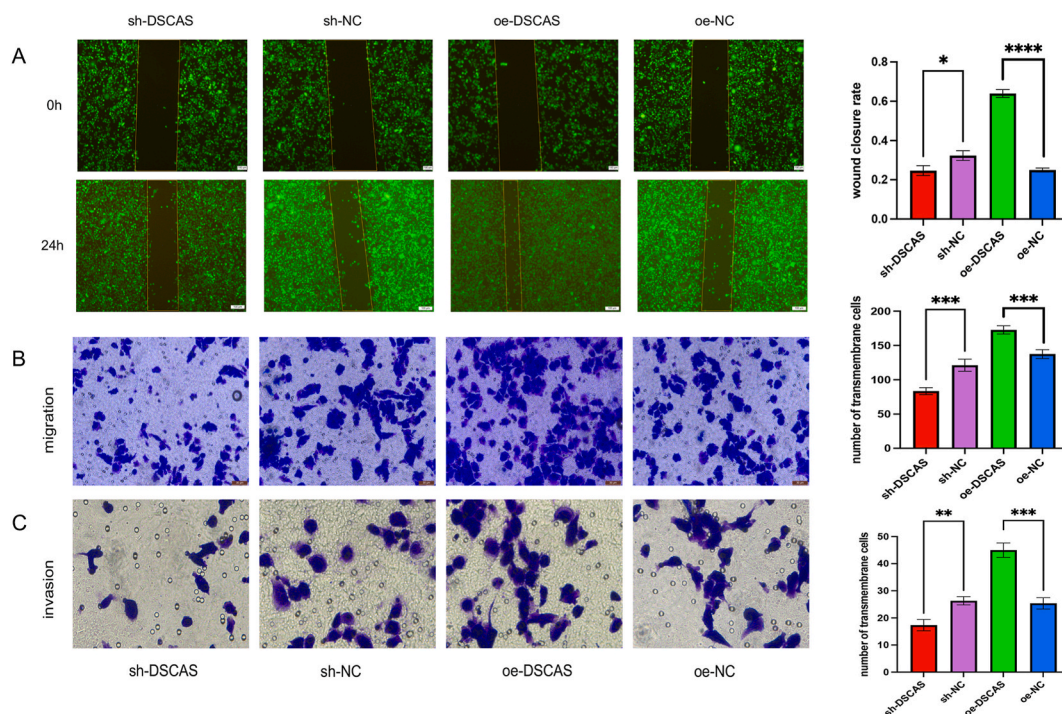


Fig. 4. Effects of modifying DSCAS on the migration and invasion of SK-MES-1 cells. (A). Wound-healing assay exhibited overexpressing DSCAS in SK-MES-1 cells promoted cell migration, while underexpressing DSCAS in SK-MES-1 cells inhibited cell migration. ($n = 3, P < .05$). Magnification: 40x. (B). Transwell for migration assay exhibited SK-MES-1 cells carrying oe-DSCAS had the most transmembrane number, while SK-MES-1 cells carrying sh-DSCAS had the least transmembrane number. ($n = 3, P < .05$). Magnification: 100x. (C). Transwell for invasion assay showed the similar result as transwell for migration assay. Magnification: 200x. ($n = 3, P < .05$). * $P < .05$, ** $P < .01$, *** $P < .001$, **** $P < .0001$ compared with control.

3.4. Regulation of DSCAS altered the sensitivity of SK-MES-1 cells to cisplatin

To elucidate the effects of DSCAS on cisplatin-sensitivity of SK-MES-1 cells, 20 μM cisplatin was added to stably transfected SK-MES-1 cells for subsequent experiments. Cell cycle assay displayed that cisplatin inhibited the growth of cell population by S phase arrest after 24h cisplatin treatment, contributing to significant increase of the fractions of cell population in S and G2/M phases together with a significant reduction in G0/G1 phase in each group. The proportion of G0/G1 phase cells in sh-DSCAS group decreased more than that in sh-NC group, and the proportion of G0/G1 phase cells in oe-DSCAS group decreased less than that in oe-NC group ($n = 3, P < .05$; Fig. 5A). IC50 of cisplatin were determined for each group using the CCK-8 for cell proliferation-toxicity assay, and the results (Fig. 5B) showed that the IC50 of cisplatin in SK-MES-1 harboring sh-DSCAS was significantly decreased (IC50: 15.30 μM vs. NC: 24.30 μM ; $n = 3, P < .05$), while the IC50 of cisplatin in SK-MES-1 cells harboring oe-DSCAS was remarkably increased (IC50: 37.20 μM vs. NC: 17.80 μM ; $n = 3, P < .05$). Taken together, these results indicated that DSCAS overexpression may increase lung cancer cells resistance to cisplatin, while DSCAS underexpression may increase lung cancer cells sensitivity to cisplatin.

3.5. DSCAS was related to cisplatin-induced apoptosis of lung cancer cells

Cisplatin induces cytotoxicity by interacting with DNA to form DNA crosslinking agents, which can cause cell apoptosis. To assess the effect of cisplatin after the regulation of DSCAS, cell apoptosis was assessed by Annexin V-APC/PI staining via flow cytometry. The results of flow cytometric analysis demonstrated that DSCAS overexpression surely suppressed cisplatin-induced early apoptosis, while DSCAS underexpression markedly promoted cisplatin-induced early apoptosis compared with NC group. ($n = 3, P < .05$; Fig. 6A–B). We also detected levels of apoptosis-related protein Bcl-2, Bax, Caspase-3, and Cleaved Caspase-3 using Western blotting. Western blotting assay indicated that compared with the control group, the expression of Bax and Cleaved Caspase-3 were remarkably declined in oe-DSCAS group and were elevated in sh-DSCAS group while Bcl-2 showed the opposite trend. ($n = 3, P < .05$; Fig. 6C–D). Caspase-3 in each group showed no statistical difference. ($n = 3, P > .05$; Fig. 6C–D). These data indicated that DSCAS overexpression suppressed cisplatin-induced apoptosis and DSCAS underexpression enhanced cisplatin-induced apoptosis in vitro.

3.6. Molecular mechanism of DSCAS that mediates the sensitivity to cisplatin in LUSC

Bioinformatics investigation revealed that the DSCAS and miR-646-3p have complimentary sequences; the 1479–1485 sites of

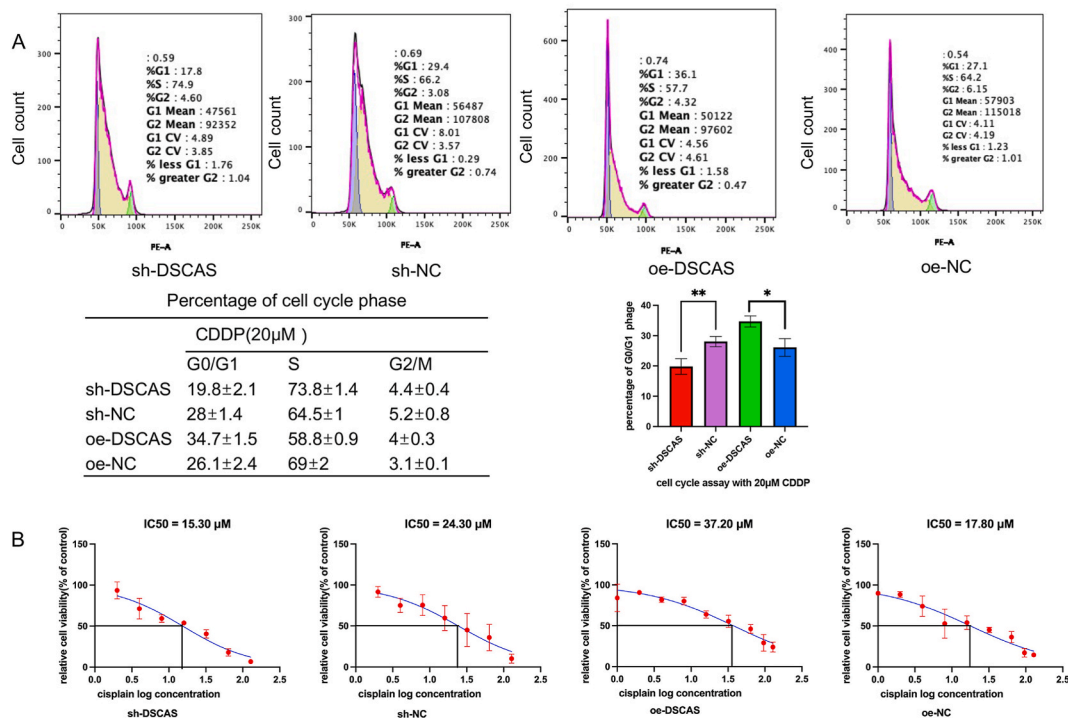


Fig. 5. Effects of regulating DSCAS on the sensitivity of cisplatin to lung cancer cells. (A). Cell cycle assay displayed that the proportion of G0/G1 phase cells in sh-DSCAS group decreased more than that in sh-NC group, and the proportion of G0/G1 phase cells in oe-DSCAS group decreased less than that in oe-NC group. ($n = 3, P < .05$). (B). CCK-8 for cell proliferation-toxicity assay indicated cisplatin IC50 of SK-MES-1 harboring oe-DSCAS was highest (37.20 μM), while cisplatin IC50 of SK-MES-1 harboring sh-DSCAS was lowest (15.30 μM). ($n = 3, P < .05$). * $P < .05$, ** $P < .01$, *** $P < .001$, **** $P < .0001$ compared with control.

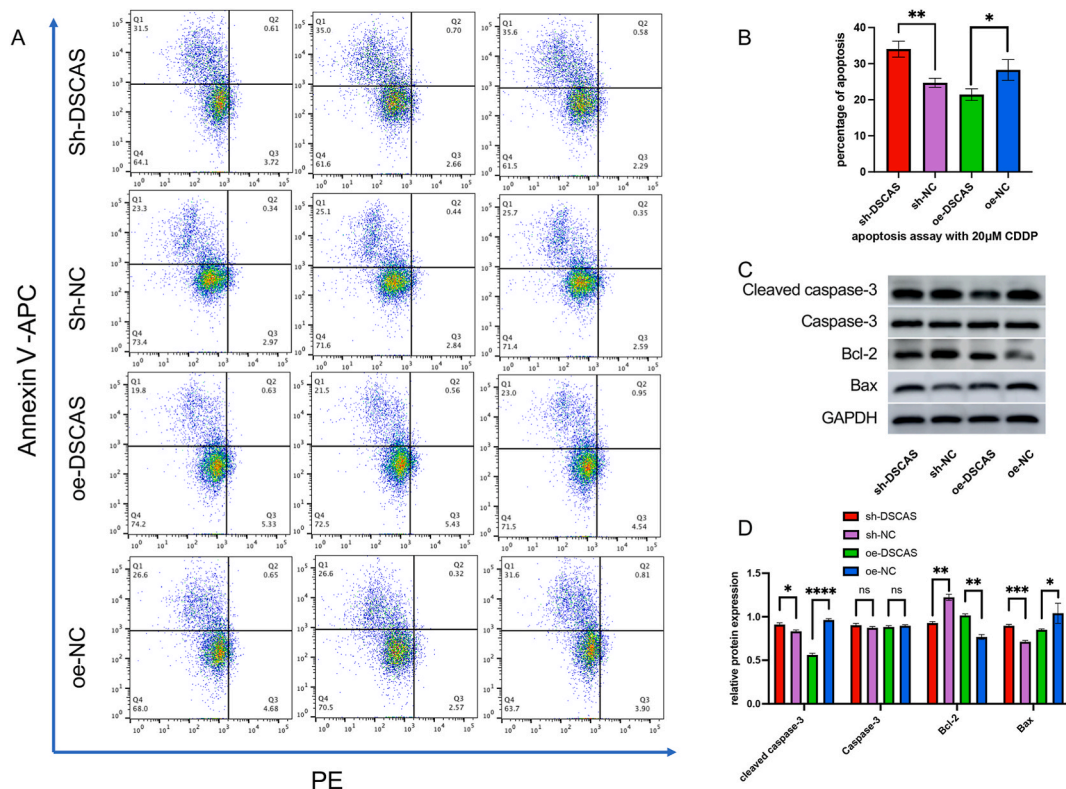


Fig. 6. Effect of cisplatin on apoptosis after DSCAS regulation. (A). After treatment with 20 μ M cisplatin for 24h, cell apoptosis was detected by flow cytometry. Q1 represents the proportion of early apoptotic cells. (B). Histogram showed the percentage of apoptotic cells in each group. ($n = 3, P < .05$). (C). The relative expression of apoptosis-related protein was detected using Western blotting. (D). Histogram displayed relative expression of apoptosis-related protein. ($n = 3, P < .05$). * $P < .05$, ** $P < .01$, *** $P < .001$, **** $P < .0001$ compared with control.

Survivin mRNA 3'UTR were complementary to miR-646-3p; the 1797–1803 sites of Bcl-2 mRNA 3'UTR were complementary to miR-646-3p. (Fig. 7A). Then the expression of miR-646-3p and mRNA of Survivin and Bcl-2 were compared in cancer and adjacent normal tissues using RT-qPCR assay, and the results displayed that compared with adjacent normal tissues, miR-646-3p expression was lower, while Survivin and Bcl-2 mRNA expression were higher in LUSC tissues. ($n = 63, P < .05$, Fig. 7B–D). Data were collected to investigate the correlation between DSCAS and miR-646-3p, DSCAS and Survivin mRNA, DSCAS and Bcl-2 mRNA, respectively. Linear trend was found from the scatter plot. It indicated that DSCAS was negatively correlated with miR-646-3p and positively correlated with Survivin and Bcl-2 mRNA. ($n = 63, P < .05; R^2 = 0.49, 0.50$ and 0.47 , respectively, Fig. 7E–G). Furthermore, we used dual luciferase reporter gene assay to verify their interaction. The results showed that the luciferase activities of SK-MES-1 cells co-transfected with miR-646-3p mimics and wild-type DSCAS vector were significantly lower than those of cells co-transfected with the mutant DSCAS vector or miR-NC. ($P < .05$; Fig. 7H). Similarly, the luciferase activities of SK-MES-1 cells co-transfected with miR-646-3p mimics and Survivin/Bcl-2 wild-type were significantly lower than the other three groups ($P < .05$; Fig. 7I–J). Based on RNA-IP and RNA Pull-down assay conducted on SK-MES-1 cells also verified that miR-646-3p could directly target lncRNA DSCAS and mRNA of Bcl-2 and Survivin ($P < .05$; Fig. 7K–N). The above experimental results demonstrated that DSCAS could bind to miR-646-3p to regulate downstream target expression; miR-646-3p negatively regulated downstream protein expression by binding to the 3'UTR of Survivin and Bcl-2 mRNA. Taken together, these data indicated that DSCAS might regulate the expression of Survivin and Bcl-2 by competitively binding miR-646-3p. To further validate the relationship between DSCAS and miR-646-3p, we also applied the RT-qPCR assay to assess miR-646-3p expression in stably transfected SK-MES-1 cell lines harboring sh-DSCAS, sh-NC, oe-DSCAS or oe-NC, respectively, and the result indicated that DSCAS negatively correlated with miR-646-3p expression. ($n = 3, P < .05$; Fig. 7O). To better understand the effect of miR-646-3p on downstream target molecules, miR-646-3p was upregulated in SK-MES-1 cells via Lipofectamine 3000 transient transfection. The transfection efficiency was confirmed by RT-qPCR assay. ($n = 3, P < .05$; Fig. 7P). Downstream target proteins, Survivin and Bcl-2, were assessed using Western blotting, which indicated that compared with their respective NC groups, Survivin and Bcl-2 were markedly declined in sh-DSCAS and miR-646-3p mimic groups. ($n = 3, P < .05$; Fig. 7Q–R). Summing up the data, our findings indicated DSCAS underexpression attenuated Survivin and Bcl-2 expression by competitively binding to miR-646-3p.

4. Discussion

Lung cancer is the malignant tumor with the highest mortality rate in China in 2022, and the prognosis of patients with LUSC is

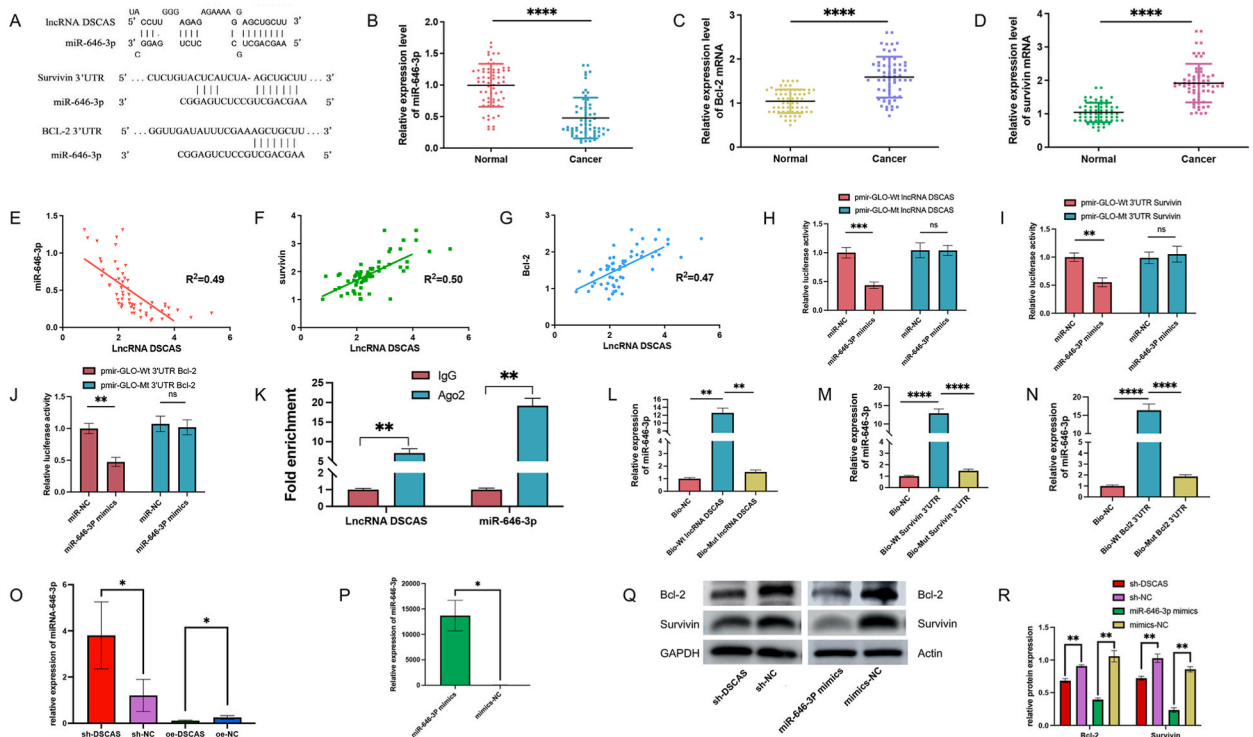


Fig. 7. Molecular mechanism of DSCAS mediating cisplatin sensitivity. (A). Bioinformatics analysis showed that DSCAS, mRNA of Bcl-2 and Survivin have targeted binding sites to miR-646-3p. (B–D). The expressions of miR-646-3p, Survivin and Bcl-2 mRNA in cancer tissues and adjacent normal tissues were compared using RT-qPCR assay. (n = 63, $P < .05$). (E). DSCAS was negatively correlated with miR-646-3p in tissues. (n = 63, $R^2 = 0.49$, $P < .05$). (F–G). DSCAS were positively correlated with Survivin and Bcl-2 mRNA. (n = 63, $R^2 = 0.50, 0.47$, respectively, all $P < .05$). (H–J). Dual luciferase reporter gene assay confirmed DSCAS, mRNA of Bcl-2 and Survivin could bind to miR-646-3p. (K–N). RNA-IP and RNA Pull-down assay confirmed DSCAS, mRNA of Bcl-2 and Survivin could bind to miR-646-3p. (O). The expression of miR-646-3p was assessed using RT-qPCR assay in stably transfected SK-MES-1 cell lines harboring sh-DSCAS, sh-NC, oe-DSCAS or oe-NC, respectively. (n = 3, $P < .05$). (P). MiR-646-3p was overexpressed in SK-MES-1 cells via Lipofectamine 3000 transient transfection and verified by RT-qPCR. (n = 3, $P < .05$). (Q). The relative expression of Bcl-2 and Survivin were detected using Western blotting assay. (R). Histogram displayed relative expression of Bcl-2 and Survivin. (n = 3, $P < .05$). * $P < .05$, ** $P < .01$, *** $P < .001$, **** $P < .0001$ compared with control.

poor [28] Targeted therapies for squamous cell lung cancer have so far been unsuccessful due to the small number of driver mutations that can be targeted [29]. Platinum-based chemotherapy and immunotherapy are the main treatment options for advanced LUSC [11]. Platinum-based chemotherapy for advanced NSCLC eventually relapses during treatment due to acquired resistance to this platinum drug [30]. Identifying the cause of chemotherapy resistance could therefore offer hope of improving the prognosis of advanced LUSC. In this study, we collected 6 cases of LUSC tissues (2 cisplatin-insensitive, 2 cisplatin-sensitive, and 2 adjacent normal tissues, respectively) and detected the differentially expressed lncRNAs by gene chip, which showed that DSCAS was higher in cisplatin-insensitive tissues than that in cisplatin-sensitive tissues. DSCAS is Homo sapiens DSC1/DSC2 antisense RNA with 553 bp. However, there are few studies on the relationship between DSCAS and cisplatin sensitivity. Hence, we collected cisplatin-sensitive and cisplatin-insensitive LUSC tissues and used LUSC cell lines to investigate the effects of DSCAS on the biological behavior and cisplatin sensitivity, making it a potential regulatory point to improve chemotherapy prognosis.

Concerning the biological processes associated with cisplatin resistance, numerous published studies have shown that almost all mechanisms that help cells survive undergo changes when resistance to this poisonous metal compound develops, including those that affect cell proliferation, apoptosis, developmental pathways, DNA damage repair, endocytosis, and so on [31]. Previous studies have shown that alterations in tumor biological behavior and cisplatin sensitivity are caused by changes in lncRNA expression levels [32]. For example, lncRNA MALAT1 modulates the biological behavior and sensitivity to cisplatin of gastric cancer cells by competitively binding miR-30e and mediating the expression level of ATG5 [33]. We therefore modulated the expression of DSCAS in the LUSC cell line (sk-mes-1) using lentiviral transfection technology and investigated changes in biological behavior, which showed that overexpression of DSCAS promoted the proliferation, migration, and invasion of LUSC cells and inhibited cell apoptosis, while underexpression of DSCAS inhibited the proliferation, migration, and invasion of LUSC cells and promoted cell apoptosis. This may be one reason why LUSC with high DSCAS expression are more likely to be resistant to cisplatin.

The mechanisms underlying cisplatin resistance are multifactorial, such as tolerance or repair of cisplatin-DNA adducts [34,35], the induction of antiapoptotic signals [36,37], the process through which drugs are actively ejected from the cell cytoplasm [38], epigenetic regulation by miRNA [39], and so on [40]. lncRNAs, recognized as key actors in drug resistance and carcinogenesis, have

recently been shown to be able to control each of these pathways [41]. Our study showed that the effect of DSCAS on cisplatin sensitivity in LUSC cells was primarily related to cisplatin-induced apoptosis. Overexpression of DSCAS inhibited cisplatin-induced apoptosis of LUSC cells, while underexpression of DSCAS promoted cisplatin-induced apoptosis of LUSC cells. Bcl-2 and Survivin are well-known anti-apoptotic genes [42]. The specific mechanism of DSCAS regulating cell apoptosis is that DSCAS, as a kind of endogenous competing RNA, sponges miR-646-3p to mediate the expression of Survivin and Bcl-2, supporting one of the lncRNA's crucial molecular mechanisms - the competitive endogenous RNA mechanism [22]. These results are consistent with previous studies showing that miR-646-3p is able to bind to the mRNA 3'UTR of Bcl-2 and survivin to regulate cell apoptosis [43]. Many studies have shown that a lncRNA can sponge specific miRNA to control the sensitivity of tumor cells to cisplatin [44,45]. The mechanistic pattern of DSCAS mediating biological behavior and cisplatin resistance in LUSC cells is illustrated in Fig. 8.

Although lots of functional experiments and mechanism exploration were performed to confirm the role of DSCAS in cisplatin resistance of LUSC, additional rescue assays and validation in vivo are still required. In addition to guiding DNA synthesis or rearranging genomes, recruiting *cis*-acting Histone-Modifying Complexes, regulating gene expression at every stage from transcription to splicing to translation, and aiding in genome organization and stability, lncRNAs perform an astonishingly wide range of other biological tasks [13]. Besides the ceRNA mechanism, other mechanisms of DSCAS in cisplatin resistance in lung cancer cells remain unclear. With the development of genomics and deep sequencing, the function of DSCAS needs to be further clarified.

5. Conclusions

DSCAS regulates biological behavior and cisplatin sensitivity in LUSC cells by competitively binding to miR-646-3p to mediate the expression of Survivin and Bcl-2, known as apoptosis-related proteins. Our findings suggest that DSCAS may serve as a potential regulatory target for chemotherapy sensitivity.

Author contributions

Guojun Zhang; Ping Li - Conceived and designed the experiments.
 Hongping Liu; Hongxia Jia: Performed the experiments, Wrote the paper.
 Yan Wang; Jiuling Cheng: Analyzed and interpreted the data.
 Ruirui Cheng; Chunya Lu: Contributed reagents, materials, analysis tools or data.

Data availability statement

The data sets generated and/or analyzed during the current study are available from the corresponding author on reasonable request.

Declaration of competing interest

The authors declare that they have no known competing financial interests or personal relationships that could have appeared to

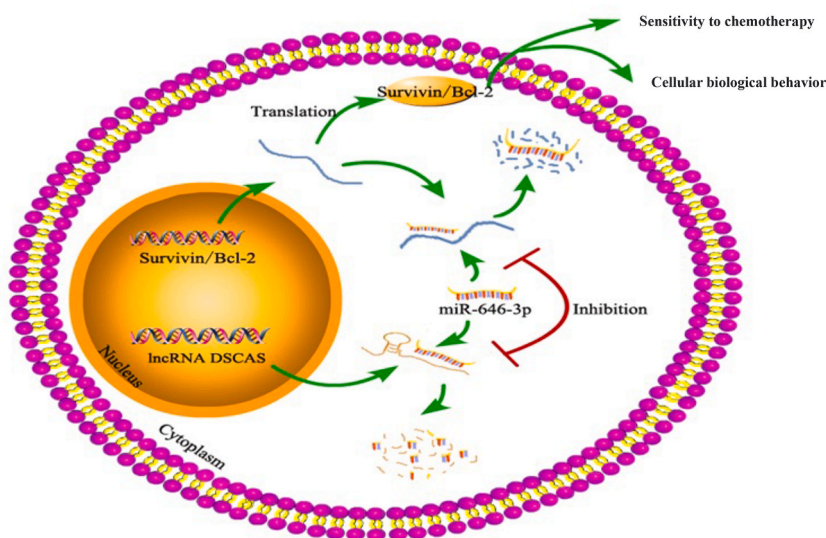


Fig. 8. Model diagram displays that DSCAS regulates the biological behavior and cisplatin sensitivity of LUSC cells by competitively binding to miR-646-3p in the form of ceRNA, and mediating the expression of Survivin and Bcl-2, which are known as apoptosis related proteins.

influence the work reported in this paper.

Acknowledgments

This study was supported by funds from National Natural Science Foundation of China and the grant ID is "81874042"; We acknowledge assistance with the access of analytical instruments from Translational Medical Center at The First Affiliated Hospital of Zhengzhou University. The funding body had no role in the design of the study, in the collection, analysis, and interpretation of the data, or in the manuscript writing.

Appendix A. Supplementary data

Supplementary data to this article can be found online at <https://doi.org/10.1016/j.heliyon.2023.e16865>.

References

- [1] R.L. Siegel, et al., Cancer statistics, 2022, *CA A Cancer J. Clin.* 72 (1) (2022) 7–33.
- [2] W. Lim, et al., The 8(th) lung cancer TNM classification and clinical staging system: review of the changes and clinical implications, *Quant. Imag. Med. Surg.* 8 (7) (2018) 709–718.
- [3] W.D. Travis, et al., The 2015 world health Organization classification of lung tumors: impact of genetic, clinical and radiologic advances since the 2004 classification, *J. Thorac. Oncol.* 10 (9) (2015) 1243–1260.
- [4] L. Friboulet, et al., The ALK inhibitor ceritinib overcomes crizotinib resistance in non-small cell lung cancer, *Cancer Discov.* 4 (6) (2014) 662–673.
- [5] A.R. Thierry, et al., Clinical validation of the detection of KRAS and BRAF mutations from circulating tumor DNA, *Nat. Med.* 20 (4) (2014) 430–435.
- [6] M. Touat, et al., Targeting FGFR signaling in cancer, *Clin. Cancer Res.* 21 (12) (2015) 2684–2694.
- [7] E.C. Nakajima, et al., FDA approval summary: sotorasib for KRAS G12C-mutated metastatic NSCLC, *Clin. Cancer Res.* 28 (8) (2022) 1482–1486.
- [8] A.C. Tan, D.S.W. Tan, Targeted therapies for lung cancer patients with oncogenic driver molecular alterations, *J. Clin. Oncol.* 40 (6) (2022) 611–625.
- [9] J.C. Soria, et al., Afatinib versus erlotinib as second-line treatment of patients with advanced squamous cell carcinoma of the lung (LUX-Lung 8): an open-label randomised controlled phase 3 trial, *Lancet Oncol.* 16 (8) (2015) 897–907.
- [10] M. Perol, et al., Randomized, phase III study of gemcitabine or erlotinib maintenance therapy versus observation, with predefined second-line treatment, after cisplatin-gemcitabine induction chemotherapy in advanced non-small-cell lung cancer, *J. Clin. Oncol.* 30 (28) (2012) 3516–3524.
- [11] D.S. Ettinger, et al., Non-small cell lung cancer, version 3.2022, NCCN clinical practice guidelines in oncology, *J. Natl. Compr. Cancer Netw.* 20 (5) (2022) 497–530.
- [12] J. Rotow, T.G. Bivona, Understanding and targeting resistance mechanisms in NSCLC, *Nat. Rev. Cancer* 17 (11) (2017) 637–658.
- [13] T.R. Cech, J.A. Steitz, The noncoding RNA revolution—trashing old rules to forge new ones, *Cell* 157 (1) (2014) 77–94.
- [14] R.C. Lee, R.L. Feinbaum, V. Ambros, The *C. elegans* heterochronic gene *lin-4* encodes small RNAs with antisense complementarity to *lin-14*, *Cell* 75 (5) (1993) 843–854.
- [15] M.K. Iyer, et al., The landscape of long noncoding RNAs in the human transcriptome, *Nat. Genet.* 47 (3) (2015) 199–208.
- [16] J.G. van Bemmel, H. Mira-Bontenbal, J. Gribnau, Cis- and trans-regulation in X inactivation, *Chromosoma* 125 (1) (2016) 41–50.
- [17] Y.H. Lin, Crosstalk of lncRNA and cellular metabolism and their regulatory mechanism in cancer, *Int. J. Mol. Sci.* 21 (8) (2020).
- [18] D.P. Bartel, MicroRNAs: genomics, biogenesis, mechanism, and function, *Cell* 116 (2) (2004) 281–297.
- [19] J.M. Engreitz, et al., The Xist lncRNA exploits three-dimensional genome architecture to spread across the X chromosome, *Science* 341 (6147) (2013), 1237973.
- [20] M. Guttman, J.L. Rinn, Modular regulatory principles of large non-coding RNAs, *Nature* 482 (7385) (2012) 339–346.
- [21] B. Ricciuti, et al., Long noncoding RNAs: new insights into non-small cell lung cancer biology, diagnosis and therapy, *Med. Oncol.* 33 (2) (2016) 18.
- [22] L. Salmena, et al., A ceRNA hypothesis: the Rosetta Stone of a hidden RNA language? *Cell* 146 (3) (2011) 353–358.
- [23] D.P. Bartel, MicroRNAs: target recognition and regulatory functions, *Cell* 136 (2) (2009) 215–233.
- [24] M.D. Paraskevopoulou, et al., DIANA-LncBase v2: indexing microRNA targets on non-coding transcripts, *Nucleic Acids Res.* 44 (D1) (2016) D231–D238.
- [25] Z.S. Ju, et al., Effect of lncRNA-*BLACAT1* on drug resistance of non-small cell lung cancer cells in DDP chemotherapy by regulating cyclin D1 expression, *Eur. Rev. Med. Pharmacol. Sci.* 24 (18) (2020) 9465–9472.
- [26] X. Liu, et al., Silence of lncRNA *UCA1* rescues drug resistance of cisplatin to non-small-cell lung cancer cells, *J. Cell. Biochem.* 120 (6) (2019) 9243–9249.
- [27] F. Guo, et al., The action mechanism of lncRNA-*HOTAIR* on the drug resistance of non-small cell lung cancer by regulating Wnt signaling pathway, *Exp. Ther. Med.* 15 (6) (2018) 4885–4889.
- [28] C. Xia, et al., Cancer statistics in China and United States, 2022: profiles, trends, and determinants, *Chin. Med. J.* 135 (5) (2022) 584–590.
- [29] T. Hayashi, et al., *RASA1* and *NF1* are preferentially Co-mutated and define a distinct genetic subset of smoking-associated non-small cell lung carcinomas sensitive to MEK inhibition, *Clin. Cancer Res.* 24 (6) (2018) 1436–1447.
- [30] L. MacDonagh, et al., Exploitation of the vitamin A/retinoic acid axis depletes *ALDH1*-positive cancer stem cells and re-sensitises resistant non-small cell lung cancer cells to cisplatin, *Trans. Oncol.* 14 (4) (2021), 101025.
- [31] D.W. Shen, et al., Cisplatin resistance: a cellular self-defense mechanism resulting from multiple epigenetic and genetic changes, *Pharmacol. Rev.* 64 (3) (2012) 706–721.
- [32] G.C. Eptaminotaki, et al., Long non-coding RNAs (lncRNAs) signaling in cancer chemoresistance: from prediction to druggability, *Drug Resist. Updates* 65 (2022), 100866.
- [33] Y.F. Zhang, et al., Propofol facilitates cisplatin sensitivity via lncRNA *MALAT1*/miR-30e/ATG5 axis through suppressing autophagy in gastric cancer, *Life Sci.* 244 (2020), 117280.
- [34] M. Macerelli, et al., Can the response to a platinum-based therapy be predicted by the DNA repair status in non-small cell lung cancer? *Cancer Treat Rev.* 48 (2016) 8–19.
- [35] B. Haynes, et al., Crosstalk between translesion synthesis, Fanconi anemia network, and homologous recombination repair pathways in interstrand DNA crosslink repair and development of chemoresistance, *Mutat. Res. Rev. Mutat. Res.* 763 (2015) 258–266.
- [36] E.J. Dean, et al., A small molecule inhibitor of XIAP induces apoptosis and synergises with vinorelbine and cisplatin in NSCLC, *Br. J. Cancer* 102 (1) (2010) 97–103.
- [37] N. Shivapurkar, et al., Apoptosis and lung cancer: a review, *J. Cell. Biochem.* 88 (5) (2003) 885–898.
- [38] G. Yang, et al., High *ABCG4* expression is associated with poor prognosis in non-small-cell lung cancer patients treated with cisplatin-based chemotherapy, *PLoS One* 10 (8) (2015), e0135576.
- [39] Y. Chen, et al., MicroRNAs as regulators of cisplatin resistance in lung cancer, *Cell. Physiol. Biochem.* 37 (5) (2015) 1869–1880.
- [40] J. Kryczka, et al., Molecular mechanisms of chemoresistance induced by cisplatin in NSCLC cancer therapy, *Int. J. Mol. Sci.* 22 (16) (2021).

- [41] M. La Montagna, L. Ginn, M. Garofalo, Mechanisms of drug resistance mediated by long non-coding RNAs in non-small-cell lung cancer, *Cancer Gene Ther.* 28 (3–4) (2021) 175–187.
- [42] M.L. Hartman, M. Czyz, Anti-apoptotic proteins on guard of melanoma cell survival, *Cancer Lett.* 331 (1) (2013) 24–34.
- [43] N.N. Chen, D.L. Chao, X.G. Li, Circular RNA has_circ_0000527 participates in proliferation, invasion and migration of retinoblastoma cells via miR-646/BCL-2 axis, *Cell Biochem. Funct.* 38 (8) (2020) 1036–1046.
- [44] Y. Jia, et al., Long non-coding RNA NORAD/miR-224-3p/MTDH axis contributes to CDDP resistance of esophageal squamous cell carcinoma by promoting nuclear accumulation of beta-catenin, *Mol. Cancer* 20 (1) (2021) 162.
- [45] J. Chen, et al., LINC00173.v1 promotes angiogenesis and progression of lung squamous cell carcinoma by sponging miR-511-5p to regulate VEGFA expression, *Mol. Cancer* 19 (1) (2020) 98.